Some Selective Serotonin Reuptake Inhibitors Inhibit Dynamin I Guanosine Triphosphatase (GTPase)

Masahiro OTOMO,[#,a] Kiyofumi TAKAHASHI,[#,a] Hiroshi MIYOSHI,[*,#,b] Kenichi OSADA,[a] Hideki NAKASHIMA,[b] and Noboru YAMAGUCHI[a]

[a] *Department of Neuropsychiatry, St. Marianna University School of Medicine; and* [b] *Department of Microbiology, St. Marianna University School of Medicine; 2–16–1 Sugao, Miyamae, Kawasaki, Kanagawa 216–8511, Japan.*

Received May 7, 2008; accepted June 6, 2008; published online June 9, 2008

Neuronal dynamin I plays a critical role in the recycling of synaptic vesicles, and thus in nervous system function. We expressed and purified dynamin I to explore potentially clinically useful endocytosis inhibitors and to examine the mechanism of their action. We estimated the IC_{50} of nineteen psychotropic drugs for dynamin I. The IC_{50} values of two selective serotonin reuptake inhibitors (sertraline and fluvoxamine) were 7.3±1.0 and 14.7±1.6 μM, respectively. Kinetic analyses revealed that fluvoxamine is a noncompetitive inhibitor of dynamin I guanosine triphosphatase (GTPase) with respect to guanosine 5′-triphosphate (GTP) and a competitive inhibitor with respect to L-phosphatidylserine (PS). Fluvoxamine may compete with PS for binding to the pleckstrin homology domain of dynamin I. On the other hand, sertraline was a mixed type inhibitor with respect to both GTP and PS. Our results indicate that sertraline and fluvoxamine may regulate the transportation of neurotransmitters by modulating synaptic vesicle endocytosis *via* the inhibition of dynamin I GTPase.

Key words dynamin; guanosine triphosphatase; endocytosis; inhibitor; selective serotonin reuptake inhibitor

Eukaryotic cells take up extracellular materials and recycle their membranes by endocytosis, which involves the formation of numerous types of membrane vesicles at the plasma membrane.[1—3] Vesicles occur in various sizes, ranging from large phagosomes, to smaller clathrin-coated vesicles, to tiny synaptic vesicles. Endocytic mechanisms have many cellular functions, including the uptake of extracellular nutrients, regulation of cell surface receptor expression and signaling, antigen presentation, and maintenance of synaptic transmission.

Synaptic transmission is dependent on the continuous reformation of synaptic vesicles *via* local membrane recycling.[4,5] Although the precise mechanisms of synaptic vesicle reformation remain a matter of debate,[6—10] there is strong evidence for a key role of the guanosine triphosphatase (GTPase) dynamin in this process,[11—15] as well as in a variety of endocytic reactions in all cell types.[12,16—19] Dynamin (Dyn) is thought to oligomerize at the neck of endocytic pits and to mediate neck constriction and fission.[11,12,14]

Receptor-mediated endocytosis (RME) and synaptic vesicle endocytosis (SVE) utilize many proteins and lipid cofactors.[3,20] SVE occurs when nerve terminals retrieve empty synaptic vesicles after stimulated exocytosis to enable refilling of these vesicles with neurotransmitters for a new round of exocytosis. Overexpression of GTPase-defective Dyn mutants inhibits both RME and SVE in a variety of cells.[21] Mammals have three dynamins with different expression patterns.[22,23] Dyn I, II and III are all found in neurons, but Dyn I is neuron-specific and is expressed much more strongly than either of the others.[23] Several observations[12,23—25] strongly suggest that Dyn I plays a dedicated and essential role in the recycling of synaptic vesicles and, thus, has a critical role in nervous system function. All dynamins have four functional domains: an N-terminal GTPase domain, a pleckstrin homology (PH) domain, a proline-rich domain (PRD), and an assembly domain also known as the GTPase effector domain (GED).[3]

L-Phosphatidylserine (PS) or phosphatidylinositol-4,5-bisphosphate (PtdIns(4,5)P2) binds the PH domain of Dyn, enhances its GTPase activity,[26,27] and induces cooperative helix assembly.[28] Myristyl trimethyl ammonium bromide (MiTMAB) is surface-active, and it alters protein–lipid interactions.[29,30] At high concentrations, MiTMAB is a cationic surfactant, as observed for other pharmacologically active cationic amphiphilic compounds, including chlorpromazine, an antipsychotic, and imipramine, an antidepressant.[31] Further, chlorpromazine is well known as an endocytosis inhibitor.[32] Thus, the inhibition of Dyn I GTPase activity by various psychotropic drugs was investigated to explore potentially clinically useful endocytosis inhibitors and to understand their mechanism of action.

MATERIALS AND METHODS

Materials PfuUltraTM II Fusion HS DNA Polymerase was purchased from Stratagene. Restriction enzymes and the DNA ligation kit ver.2 was purchased from Takara Bio Co., Ltd. TALON Metal Affinity Resin was purchased from Clontech Co., Ltd. The Mono Q 5/50 GL column was purchased from Amersham Biosciences Co., Ltd. PET21a expression vectors and *Escherichia coli* Rosetta2 (DE3) were purchased from Merck Co., Ltd. Quant-iT Protein Assay kit and Thermo-X reverse transcriptase were purchased from Invitrogen. Other chemicals in this study were of analytical or higher grade.

Construction of Expression Vector for *Mus musculus* Dyn I and GTPase Domain of Dyn I Three fragments of the Dyn I gene (gi: 116063569) were obtained by PCR from mouse brain cDNA, which was synthesized by Thermo-X reverse transcriptase. The GTPase domain (amino acid residues (aa). 1—230) of Dyn I was amplified by using primer 1 (5′-GGAATTCAGATCTCATATGGGCAACC-

* To whom correspondence should be addressed. e-mail: hmiyoshi@marianna-u.ac.jp
# These authors contributed equally to this work.

GCGGCATGGAA-3′) and primer 2 (5′-GGAATTC-CTCGAGACCTCTGCGCAAAGGGAGCAG-3′). The amplified gene was digested with *Nde* I and *Fsp* I. The middle domain (aa. 228-519) of Dyn I was amplified by using primer 3 (5′-GGAATTCATATGCGCAGAGGTTACATC-GGCG-3′) and primer 4 (5′-GGAATTCTCGAGCTTTC-GAATGACCTGGTTCCCTG-3′). The amplified gene was digested with *Fsp* I and *Bst* BI. PH-PRD domain (aa. 517—864) of Dyn I was amplified by using primer 5 (5′-GGAATTCATATGATTCGAAAGGGGTGGTTGACC-3′) and primer 6 (5′-GGAATTCTTAAGCCTCGAGTAAGTC-TAAGAGGGGAGCCT-3′). The amplified gene was digested with *Bst* BI and *Xho* I. All of the digested products were ligated into *Nde* I and *Xho* I sites in pET21a to create an expression vector for polyhistidine segment 6 residues in length (His_6) tag fused to the C-terminus of Dyn I (Dyn-His_6). Primer 1 and primer 2 were employed for PCR, and the product was digested with *Nde* I and *Xho* I, and ligated into the same sites in pET21a to create an expression vector for His_6 tag fused to the C-terminus of the GTPase domain of Dyn I. These expression vectors were named pETDyn1 and pET-DynGTP, respectively. Successful construction of all expression vectors was confirmed by DNA sequencing.

Expression and Purification of Dyn-His_6 *E. coli* Rosetta2 (DE3) cells were transformed with each of pET-Dyn1 and pETDynGTP. Cells were cultured in 6 l of LB medium containing 100 $\mu g\,ml^{-1}$ ampicillin (and 20 $\mu g\,ml^{-1}$ chloramphenicol at 37 °C. At an A_{600} of 0.5, expression was induced for 3 h with 300 μM isopropyl 1-thio-β-D-galactoside, after which cells were harvested by centrifugation. Subsequent steps were performed at 4 °C. The cell pellet was resuspended in 60 ml of Buffer A (50 mM NaH_2PO_4 pH 8.0, 300 mM NaCl, 10 mM imidazole), then disrupted by sonication, and the lysate was centrifuged.

The supernatant was applied to a 1 ml TALON Metal Affinity Resin column equilibrated with Buffer A. The column was washed three times with 10 ml of Buffer B (50 mM NaH_2PO_4 pH 8.0, 300 mM NaCl, 20 mM imidazole), and the bound protein was eluted with 7 ml of Buffer C (20 mM NaH_2PO_4 pH 8.0, 300 mM NaCl, 250 mM imidazole). The eluate was further purified to homogeneity on a MonoQ column, and finally dialyzed against Buffer D (10 mM Tris–HCl pH 8.0, 150 mM NaCl). The purified Dyn-His_6 and GTPase domain were characterized by SDS-PAGE. Protein concentration was determined with a Quant-iT Protein Assay kit (Invitrogen).

MiTMAB and Psychotropic Drugs Myristyl trimethyl ammonium bromide (MiTMAB), 5*H*-dibenz[*b*,*f*]azepine-5-carboxamide (carbamazepine), 10,11-dihydro-5-[3-(methylamino)propyl]-5*H*-dibenz[*b*,*f*]azepine monohydrochloride (desipramine), 4-[4-(4-chlorophenyl)-4-hydroxy-1-piperidyl]-1-(4-fluorophenyl)butan-1-one (haloperidol) and (1*S*)-*cis*-4-(3,4-dichlorophenyl)-1,2,3,4-tetrahydro-*N*-methyl-1-naphthalenamine (sertraline) were from Wako Pure Chemical Industries. *N*-Methyl-3-phenyl-3-[4-(trifluoromethyl)phenoxy]propan-1-amine (fluoxetine), 3-(9-chloro-5,6-dihydrobenzo[*b*][1]benzazepin-11-yl)-*N*,*N*-dimethylpropan-1-amine, (clomipramine), *N*-methyl-9,10-ethanoanthracene-9(10*H*)-propanamine (maprotiline), 3-(2-chloro-10*H*-phenothiazin-10-yl)-*N*,*N*-dimethylpropan-1-amine (chlorpromazine) and 1-[3-(dimethylamino)propyl]-1-(4-fluorophenyl)-1,3-dihydro[2]benzofuran-5-carbonitrile (citalopram) were from Sigma-Aldrich. *N*-[(1-Ethylpyrrolidin-2-yl)methyl]-2-methoxy-5-sulfamoylbenzamide (sulpiride), 2-((8-chlorodibenzo(*b*,*f*)thiepin-10-yl)oxy)-*N*,*N*-dimethylethylamine (zotepine) and *N*-(2-diethylaminoethyl)-2-methoxy-5-methylsulfonylbenzamide (tiapride) were from Astellas Pharma Inc. Methyl 2-phenyl-2-(2-piperidyl)acetate (methylphenidate) and 3-(5,6-dihydrobenzo[*b*][1]benzazepin-11-yl)-*N*,*N*-dimethylpropan-1-amine (imipramine) were from Novartis Pharma K.K. 1,2,3,4,10,14b-Hexahydro-2-methyldibenzo[*c*,*f*]pyrazino[1,2-*a*]azepine (mianserin) was from Organon, (1*R*,2*R*)-2-(aminomethyl)-*N*,*N*-diethyl-1-phenylcyclopropane-1-carboxamide (milnacipran) was from Asahi Kasei Pharma and, (3*S*-*trans*)-3-((1,3-benzodioxol-5-yloxy)-methyl)-4-(4-fluorophenyl)piperidine (paroxetine), was from GlaxoSmithKline K.K. 2-[(5-Methoxy-1-[4-(trifluoromethyl)phenyl]pentylidene)amino]oxyethanamine (fluvoxamine) was from Solvay Seiyaku K.K. and 3-(10,11-dihydro-5*H*-dibenzo[*a*,*d*]cyclohepten-5-ylidene)-*N*-methyl-1-propanamine (nortriptyline) was from Dainippon Sumitomo Pharma Co., Ltd. The drugs and MiTMAB were made up as stock solutions in 100% DMSO or 50% (v/v) DMSO, 30 mM Tris–HCl pH 7.4 and diluted in 30 mM Tris–HCl pH 7.4 prior to use in assay. Stocks were stored at −20 °C for up to several months.

GTPase Assay The Malachite Green GTPase assay was used for the sensitive colorimetric detection of orthophosphate (Pi) according to the method reported by Quan *et al.*[33,34] Purified 20 nM Dyn-His_6 (diluted in dynamin diluting buffer: 6 mM Tris–HCl, 20 mM NaCl, 0.02% Tween 80, pH 7.4) was incubated in GTPase buffer (10 mM Tris–HCl, 10 mM NaCl, 2 mM Mg^{2+}, 0.05% Tween 80, pH 7.4, 1 μg/ml leupeptin and 0.1 mM PMSF) and guanosine 5′-triphosphate (GTP) 0.3 mM in the presence of test compound for 30 min at 30 °C. The final assay volume was 40 μl. The assay was conducted in round-bottomed 96-well plates. The incubations of the plate were performed in a dry heating block with shaking at 300 rpm (Eppendorf Thermomixer). Dynamin activity was measured as phospholipid release stimulated with addition of different concentrations of PS liposomes. The reaction was terminated with 10 μl of 0.5 M EDTA pH 8.0. To each well was added 150 μl of Malachite Green solution (2% (w/v) ammonium molybdate tetrahydrate, 0.15% (w/v) malachite green and 1 M HCl: the solution was passed through 0.45 μm filters. Color was allowed to develop for 20 min, and the absorbance of samples in each plate was determined on a microplate spectrophotometer (Wallac 1420 ARVOsx from PerkinElmer) at 650 nm. Phosphate release was quantified by comparison with a standard curve of sodium dihydrogen orthophosphate monohydrate which was run in each experiment. KaleidaGraph 4.0 (Synergy Software) was used for plotting data points and analysis of enzyme kinetics using non-linear regression. The curves were generated using the Michaelis–Menten equation $v = V_{max}[S]/(K_m + [S])$ where S=PS activator or GTP substrate. After the V_{max} and K_m values were determined, the data were transformed using the Lineweaver–Burke equation $1/v = 1/V_{max} + (K_m/V_{max}) \cdot (1/[S])$.

RESULTS

Recombinant Dyn I from *E. coli* Has GTPase Activity

Although native Dyn I and recombinant Dyn I from the baculovirus expression system have been employed to investigate the GTPase activity of Dyn I,[34,35] it has not previously been confirmed that recombinant Dyn I from *E. coli* shows GTPase activity. We expressed and purified dynamin I with a His_6 tag fused to the C-terminus (Dyn-His_6) and the GTPase domain of Dyn I from *E. coli* Rosetta2 (DE3) with a His_6 tag fused to the C-terminus by transforming the cells with pET-Dyn1 and pETDynGTP (Fig. 1A). Purified Dyn-His_6 hydrolyzed GTP and released orthophosphate Pi time-dependently. In contrast, release of Pi was not observed in the case of the purified GTPase domain of Dyn I (Fig. 1B). These results clearly show that purified Dyn-His_6 from *E. coli* has GTPase activity, while the GTPase domain of Dyn I alone does not.

Some Selective Serotonin Reuptake Inhibitors (SSRIs) Inhibit the GTPase Activity of Dyn I The IC_{50} values of MiTMAB (used as a standard inhibitor of Dyn I) and nineteen psychotropic drugs were estimated as shown in Table 1. MiTMAB inhibited Dyn-His_6 GTPase with an IC_{50} of $24.1\pm9.4\,\mu M$ in this study. Quan *et al.* reported an IC_{50} value of $3.1\pm0.2\,\mu M$,[33] which is rather different from that determined here. This discrepancy may be explained by the difference between native Dyn I from sheep brain used in their study, and recombinant Dyn-His_6 from *E. coli* used in ours. Therefore, we evaluated the Dyn I inhibitory activity of the nineteen psychotropic drugs by comparing their IC_{50} values with that of MiTMAB in the same system.

Serotonin/noradrenaline reuptake inhibitor (milnacipran), anticonvulsant (carbamazepine) and the antipsychotics (chlorpromazine, haloperidol, sulpiride, zotepine and tiapride) all showed little inhibition of dynamin I GTPase activity compared with MiTMAB (Table 1). However, the IC_{50} values for two antidepressants (clomipramine and maprotiline) and two SSRIs (fluoxetine and paroxetine) were greater than or similar to the IC_{50} for MiTMAB (Table 1). It is noteworthy that the two SSRIs showed lower IC_{50} values (7.3 ± 1.0 mM for sertraline and $14.7\pm1.6\,\mu M$ for fluvoxamine, Table 1) than MiTMAB. The full concentration response curves are shown in Fig. 2. Other psychotropic drugs did not inhibit dynamin I GTPase activity (Table 1).

How Do Sertraline and Fluvoxamine Inhibit Dynamin I GTPase? To investigate whether sertraline and fluvoxamine interfere with the activity of dynamin I GTPase, kinetic analysis of dynamin I GTPase activity in the presence of various concentrations of PS liposomes or GTP was conducted (Fig. 3).

Kinetic analysis with increasing concentrations of GTP revealed that the maximal velocity of dynamin I GTPase activity, V_{max}, was 573 nmol/mg/min and the Michaelis–Menten constant, K_m, was $25.3\,\mu M$, as calculated from the line for $0\,\mu M$ fluvoxamine in Fig. 3B. In the presence of sertraline or fluvoxamine, the V_{max} decreased and K_m increased with increasing concentrations of SSRI. The Lineweaver–Burke plots show mixed type inhibition (Figs. 3A—D).

With PS liposomes, the V_{max} was 593 nmol/mg/min, and the K_m was $0.445\,\mu M$, as calculated from the line for $0\,\mu M$ fluvoxamine in Fig. 3F. In the presence of fluvoxamine, there was no effect on V_{max}. On the other hand, K_m increased with increasing concentrations of fluvoxamine. These data show that fluvoxamine competes with PS for binding to Dyn I.

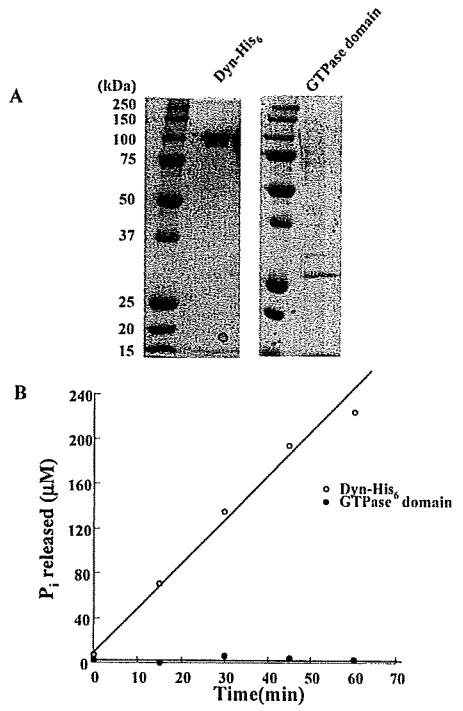

Fig. 1. Dyn-His_6 Has GTPase Activity

(A) Purified Dyn-His_6 and GTPase domain of dynamin I with a His_6 tag. The purified proteins were resolved by 15% SDS-PAGE and stained with Coomassie Brilliant Blue. (B) The time–course of GTPase activities. GTPase activities of 20 nM Dyn-His_6 and the GTPase domain were measured at 30 °C, as described under Materials and Methods. The concentration of Pi released is plotted as a function of time.

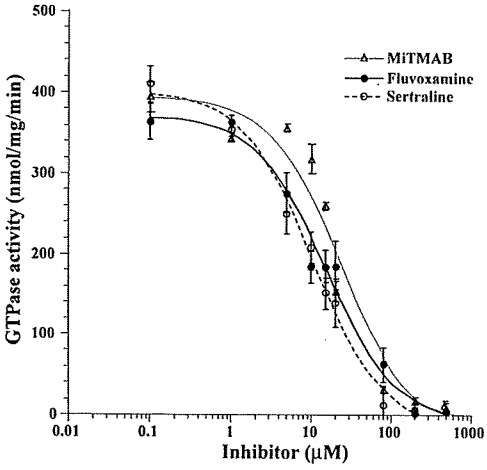

Fig. 2. Sertraline and Fluvoxamine Inhibit the GTPase Activity of Dynamin I

The GTPase activity of purified Dyn-His_6 (20 nM) was determined in the presence of various concentrations of MiTMAB, sertraline or fluvoxamine. L-Phosphatidylserine (PS, $5.0\,\mu M$)-stimulated activity was measured. All results are representative of at least 2 independent experiments.

Lineweaver–Burke double reciprocal plots indicated competitive inhibition with respect to PS (Fig. 3F). In the presence of sertraline, V_{max} decreased and K_m increased with increasing concentrations of sertraline. The Lineweaver–Burke plots show mixed type inhibition (Figs. 3E—H).

DISCUSSION

Ramachandran *et al.* reported that the Dyn middle domain

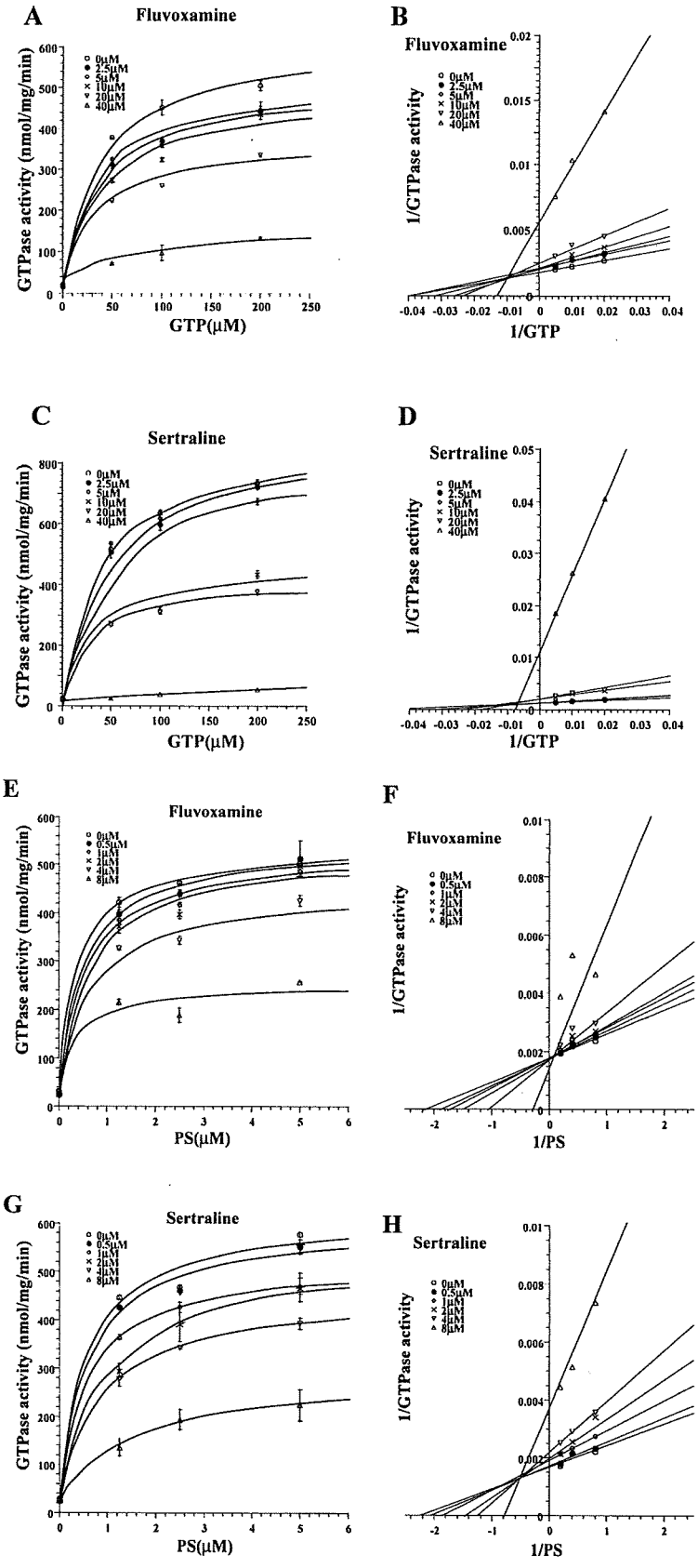

Fig. 3. Sertraline Does Not Compete with PS, But Fluvoxamine Competes with PS

The effect of fluvoxamine is shown in Michaelis–Menten (A) and Lineweaver–Burke (B) plots of the GTPase activity of purified Dyn-His_6 (20 nM) with increasing concentrations of GTP and a fixed concentration of PS (5.0 μM). The panels (C) and (D) show Michaelis–Menten and Lineweaver–Burke plots of the GTPase activity in the case of sertraline. The panels (E) and (F) show Michaelis–Menten and Lineweaver–Burke plots of the GTPase activity of purified Dyn-His_6 in the absence and presence of the indicated concentrations of fluvoxamine with increasing concentrations of PS liposomes and a fixed concentration of GTP (300 μM). The panels (G) and (H) show Michaelis–Menten and Lineweaver–Burke plots of the GTPase activity in the case of sertraline. All results are representative of at least 2 independent experiments.

Table 1. Inhibition of Dynamin I GTPase Activity by MiTMAB and Phychotropic Drugs

	Compound	Structure	IC_{50} (μM)
1	Myristyl trimethyl ammonium bromide (MiTMAB)	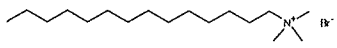	24.1±9.4
2	3-(2-Chloro-10*H*-phenothiazin-10-yl)-*N*,*N*-dimethyl-propan-1-amine (chlorpromazine)	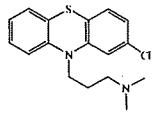	47.2±23.1
3	4-[4-(4-Chlorophenyl)-4-hydroxy-1-piperidyl]-1-(4-fluorophenyl)-butan-1-one (haloperidol)	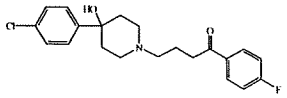	>100
4	*N*-[(1-Ethylpyrrolidin-2-yl)methyl]-2-methoxy-5-sulfamoyl-benzamide (sulpiride)	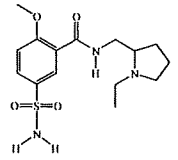	>100
5	2-((8-Chlorodibenzo(*b*,*f*)thiepin-10-yl)oxy)-*N*,*N*-dimethylethylamine (zotepine)	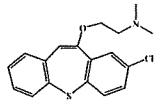	37.2±17.3
6	*N*-(2-Diethylaminoethyl)-2-methoxy-5-methylsulfonyl-benzamide (tiapride)	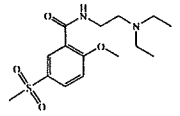	>100
7	Methyl 2-phenyl-2-(2-piperidyl)acetate (methylphenidate)	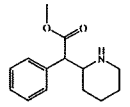	>100
8	3-(5,6-Dihydrobenzo[*b*][1]benzazepin-11-yl)-*N*,*N*-dimethylpropan-1-amine (imipramine)	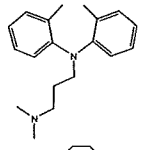	>100
9	3-(9-Chloro-5,6-dihydrobenzo[*b*][1]benzazepin-11-yl)-*N*,*N*-dimethylpropan-1-amine (clomipramine)	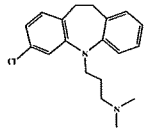	29.9±5.9
10	10,11-Dihydro-5-[3-(methylamino)propyl]-5*H*-dibenz [*b*,*f*]azepine monohydrochloride (desipramine)	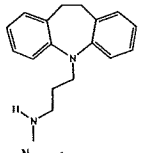	>100
11	*N*-Methyl-9,10-ethanoanthracene-9(10*H*)-propanamine (maprotiline)	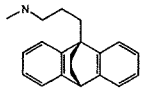	21.1±3.6
12	3-(10,11-Dihydro-5*H*-dibenzo[*a*,*d*]cyclohepten-5-ylidene)-*N*-methyl-1-propanamine (nortriptyline)	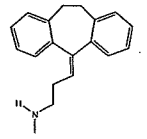	64.0±38.0
13	1,2,3,4,10,14b-Hexahydro-2-methyldibenzo(*c*,*f*)pyrazino[1,2-*a*]azepine (mianserin)	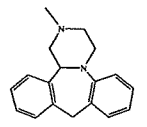	>100
14	5*H*-Dibenz[*b*,*f*]azepine-5-carboxamide (carbamazepine)	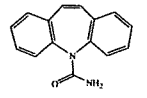	>100
15	(1*R*,2*R*)-2-(Aminomethyl)-*N*,*N*-diethyl-1-phenyl-cyclopropane-1-carboxamide (milnacipran)	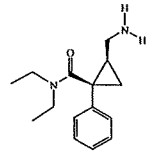	>100

Table 1. (Continued)

	Compound	Structure	IC_{50} (μM)
16	1-[3-(Dimethylamino)propyl]-1-(4-fluorophenyl)-1,3-dihydro[2]benzofuran-5-carbonitrile (citalopram)	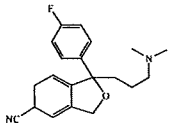	>100
17	*N*-Methyl-3-phenyl-3-[4-(trifluoromethyl)phenoxy]-propan-1-amine (fluoxetine)	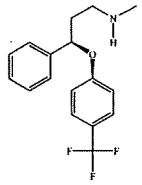	33.4±12.2
18	(3*S*-*trans*)-3-((1,3-Benzodioxol-5-yloxy)methyl)-4-(4-fluorophenyl)-piperidine (paroxetine)	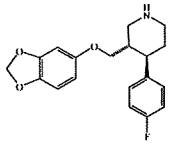	23.4±8.0
19	(1*S*)-*cis*-4-(3,4-Dichlorophenyl)-1,2,3,4-tetrahydro-*N*-methyl-1-naphthalenamine (sertraline)	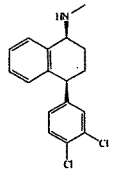	7.3±1.0
20	2-[(5-Methoxy-1-[4-(trifluoromethyl)phenyl]pentylidene)amino]oxyethanamine (fluvoxamine)	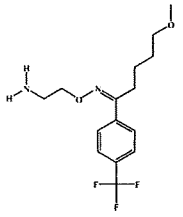	14.7±1.6

is necessary for tetramerization and higher-order self-assembly.[35] Dyn exhibits GTPase activity upon self-assembly and undergoes appreciable conformational changes during its GTP hydrolysis cycle.[28,36] These observations are consistent with our finding that the GTPase domain of Dyn I did not show GTPase activity. On the other hand, purified Dyn-His_6 from *E. coli* did show GTPase activity.

It is known that Dyn I is dephosphorylated by the calcium-dependent phosphatase calcineurin[37] and is subsequently rephosphorylated by cyclin-dependent kinase 5 (cdk5) on Ser774 and Ser778 during SVE.[38,39] Although Dyn-His_6 from *E. coli* would not have undergone post-translational modification, such as phosphorylation, it should be suitable for the present purpose, since it retains GTPase activity at least.

The IC_{50} values for sertraline and fluvoxamine (7.3± 1.0 μM and 14.7±1.6 μM, Table 1) were less than the IC_{50} of MiTMAB (Table 1), so these SSRIs are inhibitors of dynamin I GTPase. The IC_{50} value of chlorpromazine was 47.2±23.1 μM (Table 1) in this study. Given that chlorpromazine is a well-known endocytosis inhibitor,[32] it seems likely that sertraline and fluvoxamine inhibit endocytosis by repressing dynamin I GTPase activity.

MiTMAB is a surface-active compound that competes with PS for binding to the dynamin I PH domain, and it is a noncompetitive inhibitor with respect to GTP.[33] Fluvoxamine showed mixed type inhibition with respect to GTP and competitive inhibition with respect to PS in this study (Fig. 3). Therefore, it seems that fluvoxamine competes with PS for binding to the dynamin I PH domain, like MiTMAB. Fluvoxamine has a methoxypentylidene group, which may behave like the alkyl chain of MiTMAB.

Sertraline showed mixed type inhibition with respect to GTP and PS (Fig. 3). We cannot explain the inhibition mechanism of sertraline from the results of this study, but it is clearly different from that of fluvoxamine.

Most of the SSRIs (fluoxetine, paroxetine, sertraline and fluvoxamine) inhibited dynamin I GTPase (Table 1). Dyn I is expressed at much higher levels than Dyn II and III in neurons, and plays a critical role in nervous system function.[23—25] We speculate that these SSRIs regulate the transportation of neurotransmitters through the modulation of the synaptic vesicle endocytosis *via* the inhibition of dynamin I GTPase.

Acknowledgements This work was supported in part by Grants-in-Aid for Scientific Research and Special Coordination Funds for Promoting Science and Technology (Leading Research Utilizing Potential of Regional Science and Technology) of the Ministry of Education, Culture, Sports, Science and Technology of the Japanese Government. The authors thank Ms. Shigemi Terakubo and Ms. Satomi Yamazaki for their technical assistance.

REFERENCES

1) McClure S. J., Robinson P. J., *Mol. Membr. Biol.*, **13**, 189—215 (1996).
2) Cousin M. A., Robinson P. J., *J. Neurochem.*, **73**, 2227—2239 (1999).

3) Cousin M. A., Robinson P. J., *Trends Neurosci.*, **24**, 659—665 (2001).
4) Murthy V. N., De Camilli P., *Annu. Rev. Neurosci.*, **26**, 701—728 (2003).
5) Sudhof T. C., *Annu. Rev. Neurosci.*, **27**, 509—547 (2004).
6) Ceccarelli B., Hurlbut W. P., Mauro A., *J. Cell Biol.*, **57**, 499—524 (1973).
7) Harata N. C., Aravanis A. M., Tsien R. W., *J. Neurochem.*, **97**, 1546—1570 (2006).
8) Heuser J. E., Reese T. S., *J. Cell Biol.*, **57**, 315—344 (1973).
9) Wienisch M., Klingauf J., *Nat. Neurosci.*, **9**, 1019—1027 (2006).
10) Granseth B., Odermatt B., Royle S. J., Lagnado L., *Neuron*, **51**, 773—786 (2006).
11) Hinshaw J. E., *Annu. Rev. Cell Dev. Biol.*, **16**, 483—519 (2000).
12) Praefcke G. J., McMahon H. T., *Nat. Rev. Mol. Cell Biol.*, **5**, 133—147 (2004).
13) Sever S., Damke H., Schmid S. L., *Traffic*, **1**, 385—392 (2000).
14) Roux A., Uyhazi K., Frost A., De Camilli P., *Nature* (London), **441**, 528—531 (2006).
15) Newton A. J., Kirchhausen T., Murthy V. N., *Proc. Natl. Acad. Sci. U.S.A.*, **103**, 17955—17960 (2006).
16) McNiven M. A., Cao H., Pitts K. R., Yoon Y., *Trends Biochem. Sci.*, **25**, 115—120 (2000).
17) Macia E., Ehrlich M., Massol R., Boucrot E., Brunner C., Kirchhausen T., *Dev. Cell*, **10**, 839—850 (2006).
18) van der Bliek A. M., Redelmeier T. E., Damke H., Tisdale E. J., Meyerowitz E. M., Schmid S. L., *J. Cell Biol.*, **122**, 553—563 (1993).
19) Herskovits J. S., Burgess C. C., Obar R. A., Vallee R. B., *J. Cell Biol.*, **122**, 565—578 (1993).
20) Le Roy C., Wrana J. L., *Nat. Rev. Mol. Cell Biol.*, **6**, 112—126 (2005).
21) Marks B., Stowell M. H., Vallis Y., Mills I. G., Gibson A., Hopkins C. R., McMahon H. T., *Nature* (London), **410**, 231—235 (2001).
22) Cook T., Mesa K., Urrutia R., *J. Neurochem.*, **67**, 927—931 (1996).
23) Ferguson S. M., Brasnjo G., Hayashi M., Wolfel M., Collesi C., Giovedi S., Raimondi A., Gong L. W., Areil P., Paradise S., O'Toole E., Flavell R., Cremona O., Miesenbock G., Ryan T. A., De Camilli P., *Science*, **316**, 570—574 (2007).
24) Cao H., Garcia F., McNiven M. A., *Mol. Biol. Cell*, **9**, 2595—2609 (1998).
25) Takei K., McPherson P. S., Schmid S. L., De Camilli P., *Nature*, **374**, 186—190 (1995).
26) Zheng J., Cahill S. M., Lemmons M. A., Fushman D., Schlessinger J., Cowburn D., *J. Mol. Biol.*, **255**, 14—21 (1996).
27) Lin H. C., Barylko B., Achiriloaie M., Albanesi J. P., *J. Biol. Chem.*, **272**, 25999—26004 (1997).
28) Stowell M. H., Marks B., Wigge P., McMahon H. T., *Nat. Cell Biol.*, **1**, 27—32 (1999).
29) Scurlock J. E., Curtis B. M., *Anesthesiology*, **54**, 265—269 (1981).
30) Schreier S., Malheiros S. V., de Paula E., *Biochim. Biophys. Acta*, **1508**, 210—234 (2000).
31) Ahyayauch H., Requero M. A., Alonso A., Bennouna M., Goni F. M., *J. Colloid Interface Sci.*, **256**, 284—289 (2002).
32) Wang L. H., Rothberg K. G., Anderson R. G., *J. Cell Biol.*, **123**, 1107—1117 (1993).
33) Quan A., McGeachie A. B., Keating D. J., van Dam E. M., Rusak J., Chau N., Malladi C. S., Chen C., McCluskey A., Cousin M. A., Robinson P. J., *Mol. Pharmacol.*, **72**, 1425—1439 (2007).
34) Quan A., Robinson P. J., *Methods Enzymol.*, **404**, 556—569 (2005).
35) Ramachandran R., Surka M., Chappie J. S., Fowler D. M., Foss T. R., Song B. D., Schmid S. L., *EMBO J.*, **26**, 559—566 (2007).
36) Chen Y. J., Zhang P., Egelman E. H., Hinshaw J. E., *Nat. Struct. Mol. Biol.*, **11**, 574—575 (2004).
37) Liu J. P., Sim A. T., Robinson P. J., *Science*, **265**, 970—973 (1994).
38) Tan T. C., Valova V. A., Malladi C. S., Graham M. E., Berven L. A., Jupp O. J., Hansra G., McClure S. J., Sarcevic B., Boadle R. A., Larsen M. R., Cousin M. A., Robinson P. J., *Nat. Cell Biol.*, **5**, 701—710 (2003).
39) Larsen M. R., Graham M. E., Robinson P. J., Roepstorff P., *Mol. Cell. Proteomics*, **3**, 456—465 (2004).

Original Article

Induction of melanocyte precursors from neural crest cells surrounding the neural tube-like structures developed *in vitro* using mouse ES cell culture

Koh-ichi Atoh[1,2], Manae S.Kurokawa[1], Hideshi Yoshikawa[1], Chieko Masuda[1], Erika Takada[1], Norio Kumagai[2] and Noboru Suzuki[1,3,*]

[1]Departments of Immunology and Medicine, [2]Department of Plastic and Reconstructive Surgery, St. Marianna University School of Medicine, Kawasaki, Japan

[3]Department of Regenerative Medicine, Institute of Advanced Medical Science, St. Marianna University Graduate School of Medicine, Kawasaki, Japan

Neural crest cells differentiate into various cell types including melanocytes. In this study, we wanted to induce neural crest cells locating outside of neural tube by culturing mouse ES cells with retinoic acid (RA) and bone morphologic protein 4 (BMP4) *in vitro*, which mimicked the appearance of neural crest cells in the fetus. Histological examination of the cell aggregates composed of ES cells treated with RA and BMP4 disclosed emergence of neural tube-like structures surrounded by slug expressing neural crest cells. We detected melanocyte associated mRNAs such as pax3, sox10, Mitf and tyrosinase by RT-PCR of the aggregates. The neural crest cells expressed KIT and tyrosinase, indicating their differentiation to the melanocyte lineage. To accelerate the melanocyte induction, the cells were further treated by stem cell factor and endothelin 3 and then were transplanted to mouse femoral quadriceps muscles. They adhered to the recipient muscle tissue and retained the characteristics of melanocyte precursors, including expression of slug, KIT, endothelin receptor B and tyrosinase. Collectively, the neural crest cells derived from ES cells have a potency to differentiate into melanocyte precursors and they may be applicable for use in certain disease conditions such as vitiligo vulgaris in future.

Rec.9/11/2006, Acc.12/18/2006, pp45-52

* Correspondence should be addressed to:
Noboru Suzuki, Departments of Immunology and Medicine, St. Marianna University School of Medicine, 2-16-1 Sugao, Miyamae-ku, Kawasaki, Kanagawa 216-8511, Japan. Phone: +81-44-977-8111(Ext.3545). Fax: +81-44-975-3315, e-mail: n3suzuki@marianna-u.ac.jp

Key words ES Cell, retinoic acid, bone morphologic protein 4, neural crest cells, melanocyte precursors

Introduction

Melanocytes are derived from neural crest cells which emigrate out of the dorsal area of the neural tube[1]. Neural crest cells (NCCs) are origins of a variety of cell types including neural cells of peripheral nervous system, craniofacial skeleton and cartilage, smooth muscle and melanocytes[2]. Expression of the zinc-finger transcriptional factors, slug and snail, is known as an early response to neural crest-inducing signal[3]. One of the *paired box* (pax) genes, pax3, is expressed in NCCs and functions in the development of neural crest derivatives[2,4,5].

In the early phase of melanocyte development from NCCs, two ligand receptor systems, stem cell factor (SCF) and its receptor KIT (encoded by c-kit), and endothelin 3 (EDN3) and its receptor endothelin receptor B (EDNRB), indispensably act for survival/differentiation and expansion/emigration of melanoblasts, respectively[6]. Pax3 and the high-mobility group box protein, Sox10, bind to the promoter region of microphthalmia-associated transcription factor (Mitf), a master transcription factor governing the differentiation of melanocytes, and regulate its expression[7-10]. Another transcription factor, lymphoid enhancer factor 1 (Lef1), interacts with β-catenin together with T cell factor and enhances the expression of Mitf. Lef1 binds to the Mitf promoter and transducing Wnt signaling[11,12]. Tyrosinase, tyrosinase related protein 1 (Tyrp1) and dopachrome tautomerase (Dct, also known as Tyrp2) are the three major enzymes of tyrosinase-related family specifically expressed in pigment cells[13]. Tyrosinase, Tyrp1 and Dct were involved in the biosynthetic pathway of melanins and all the three gene promoters contain an E-box motif, bound by Mitf, suggesting importance of Mitf in pigment cell specific gene regulation.

Embryonic stem (ES) cells are pluripotent cells capable of differentiating into cells of all the three germ layers[14-16]. They have potent self-renewing capability for providing unlimited numbers of cells. Thus, ES cells are a possible candidate as cell source for transplantation therapy. In our previous study, we induced neural tube-like structures from mouse ES cells *in vitro* and obtained NCCs expressing slug and snail that resided at periphery of the tube-like structures[17]. The NCCs efficiently expanded by the addition of bone morphological protein (BMP) 4.

In this study, we induced differentiation of melanocyte precursors from the NCCs residing around the neural tube-like structures. They expressed the transcription factors and proteins essential for the melanocyte development, and adhered to mouse tissue when transplanted. The melanocyte precursors obtained *in vitro* are an excellent tool for analysis of melanocyte differentiation and for treatment of hypomelanoses such as vitiligo vulgaris.

Materials And Methods

Induction of melanocyte precursors from mouse ES cells

Mouse ES cell line, E14.1; a kind gift of Dr Klaus Rajewsky, Cologne University (Passage number 11-15, normal karyotype) was used for this study. Undifferentiated ES cells were cultured on the mitomycin C treated mouse fetal fibroblasts in DMEM supplemented with 2 mM glutamine, 0.1 mM β-mercaptoethanol, 1 x non-essential amino acids, 1 x pyruvate, 15% fetal calf serum and 1000 U/ml of recombinant mouse leukemia inhibitory factory (LIF, Life Technologies, Grand Island, NY).

We induced melanocyte differentiation from the ES cells by treating the cells with all-*trans* retinoic acid (RA, Sigma-Aldrich, Saint Louis, MO) and recombinant human BMP4 (R&D systems, Minneapolis, MN). Undifferentiated ES cells were cultured in DMEM supplemented with 15 % FCS without LIF (We defined the starting day of this LIF-depleted culture as Day0, Fig.1). Four days later, floating cell aggregates, embryoid bodies (EB), were transferred onto fresh dishes and 1 μM RA was added at Day 4 and Day 6 (Fig. 1, arrows). At Day 8, the cell aggregates were re-plated and further cultured in FCS-depleted medium consisting of DMEM/F12, N2 supplement and fibronectin for up to Day 16. 10ng/ml BMP4 were added to the cell culture at Day 10, Day 12 and Day 14 (Fig.1, downward arrowheads). Alternatively, 10ng/ml BMP4, 10ng/ml SCF (R&D systems) and 10nM EDN3 (Sigma) were added to the cell culture for the cell transplantation at Day 10 (Fig.1, the upward arrowhead).

RT-PCR

The cultured cell aggregates with RA and BMP4 were recovered at Day 10, 14 and 16. Alternatively, the cell aggregates cultured with RA, BMP4, SCF and EDN3 were recovered at Day 12 and 14. Total RNA was extracted by AGPC method and cDNA was synthesized[18]. PCR program started with preheating at 94℃ for 120 sec and then cycled 35 times of the following three steps: denaturing at 94℃ for 30 sec, annealing at 54℃ for 30 sec, and elongation at 72℃ for 60 sec. Primers used in this study were as follows; βactin (expected size: 450bp), sense gatgacgatatcgctgcgctg, antisense gtacgaccagaggcatacagg; slug (491bp), sense ggtcaagaaacatttcaacg, antisense catattcctgtcacagtac; snail (219bp), sense gtggaaaggccttctctaggc, antisense cagactcttggtgcttgtgg; pax3 (448bp) sense ccaggatgatgcggcccggcccggg, antisense aggatgcggctgatagaactcactg; c-kit (268bp) sense gacgtcatgaagacttgctg, antisense acagcagcaaagcctgttgg; EDNRB (701bp) sense cgagctgttgcttcttggagtag, antisense aacggaagttgtcatatccgtgat; Lef1 (302bp) sense cacctacagcgacgagcact, antisense cgtgttgaggcttcacgtgc; Sox10 (536bp) sense acctttgatgtgactgagctggacc, antisense cccctctaaggtcgggatatggggt; Mitf (202bp) sense agagcagggcagagagtgag, antisense ccctggttgctgtagaggtc; Tyrp1 (199bp) sense tttcactgatgcggtctttg, antisense ctgacctggccattgaactt; Dct (204bp) sense accctgtgtttgtggtcctc, antisense cggcgtaattgtagccaagt; tyrosinase (198bp) sense aggatgctgggctgagtaag, antisense catgaagcaccagggtttct. A part of the above molecules were also examined their expression in undifferentiated ES cells. NCC-

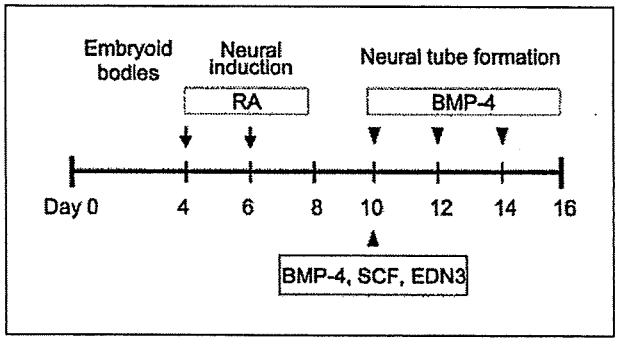

Fig.1 Cell culture protocol for differentiation of melanocyte precursors from ES-derived NCCs

Mouse ES cells were transferred to non-coated dishes on Day 0 and were cultured for four days to form EBs. RA was added twice on Day4 and Day6 to induce neural differentiation. On Day8, the EBs were transferred into FCS-depleted medium containing N2 supplement and fibronectin. BMP4 was added to the cell culture on Day10, 12 and 14. Alternatively, SCF and EDN3 together with BMP4 were added on Day10 for the cell transplantation experiment.

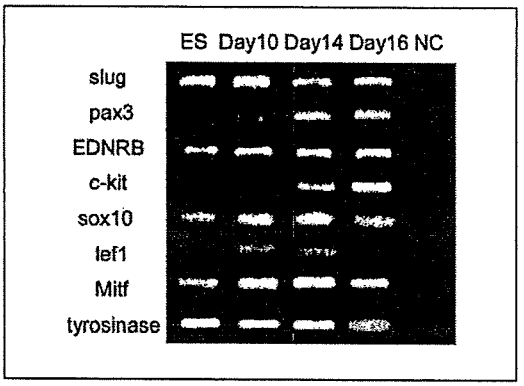

Fig.2 mRNA expressions of the melanocyte precursors induced by RA and BMP4

ES cells were first treated by RA on Day 4 and Day 6, and then treated by BMP4 on Day 10, 12 and 14 (see Fig.1). The cells were further cultured up to Day 16. Expression of mRNAs associated with the neural crest and melanocyte differentiation was studied by RT-PCR. The expression was also examined using un-differentiated ES-derived cDNAs (ES). De-ionized water was used as PCR template for negative control study (NC).

melan5 cells were kindly provided by Prof. Masako Mizoguchi in Department of Dermatology, St. Marianna University School of Medicine and cDNA of the cells was used for the positive control.

Immunohistochemistry

The cell aggregates with RA and BMP4 were recovered at Day 16, were quickly frozen and were sliced as 5 μm thickness of the tissue. After fixing with 4% paraformaldehide, the tissue sections were stained with the primary antibodies specific for slug (Santa Cruz Biotechnology, Santa Cruz, CA; dilution for staining, 1:100), Kit (Becton Dickinson, San Jose, CA; 1:400) and tyrosinase. The antibody specific for tyrosinase was kindly provided by Prof. Vincent Hearing in Laboratory of Cell Biology, National Institutes of Health (dilution for staining, 1:500). Reactivity was visualized with 3-amino-9-ethylcarbazole solution and the sections were counterstained with hematoxylin.

Transplantation of melanocyte precursors to mouse femoral quadriceps muscles

6-8 week old C57BL/6 mice were randomly divided into two groups. The cell aggregates cultured in the presence of RA, BMP4, SCF and EDN3 were harvested at day 14 and treated with trypsin. 1 x 10^6 of the cells was suspended in 10 μl PBS and injected into the femoral quadriceps muscles of mice in one group. The same volume of PBS was similarly injected in the other group. The muscles were recovered five days after the injection. Totally 8 mice were transplanted the cells.

Immunofluorescence staining

Tissue samples of the femoral quadriceps muscles were stained with two color immunofluorescence using antibodies for KIT, slug, tyrosinase and EDNRB (Biogenesis, Kingston, NH; dilution for staining, 1:50). Reactivity was then visualized using the following two systems: biotin-conjugated secondary antibodies (DakoCytomation, Glostrup, Denmark; 1:400)/Streptavidin-conjugated Cy3 (Jackson ImmunoResearch, West Grove, PA; 1:6000) and FITC-conjugated secondary antibodies (NBA Kit, Zymed, South San Francisco, CA; ready to use)/antiFITC-conjugated Alexa488 (Invitrogen/Molecular Probe, Carlsbad, CA; 1:400). Fluorescence was recorded by a confocal microscope (LSM510 META, Carl Zeiss, Jena, Germany).

Results

The aim of our study is to induce melanocyte precursors from NCCs that have been differentiated from mouse ES cells. We previously developed neural tube-like structures surrounded by slug positive NCCs using ES cell culture. ES cells were induced to differentiate into neural lineage by the stimulation with RA

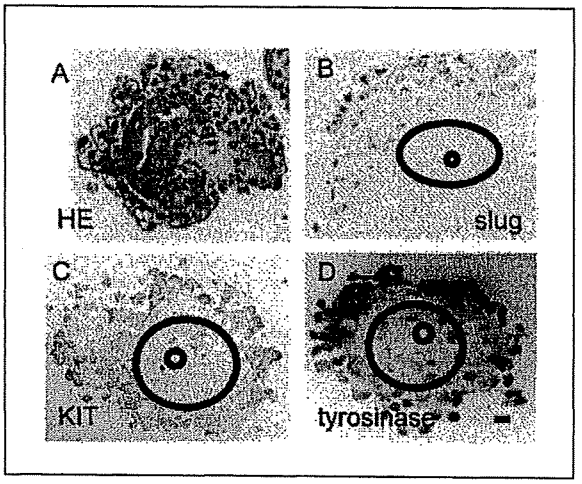

Fig.3 Expression of melanocyte related proteins in the melanocyte precursors derived from NCCs that had appeared around the neural tube-like structures *in vitro*

(A) HE staining of a cell aggregate at Day 14 treated by RA and BMP4 (three times). The neural tube-like structure was surrounded by the cells.
(B) A representative result of a cell aggregate at Day 16 containing a neural tube-like structure (double circles). Cells surrounding the tube-like structure expressed slug in their nuclei.
(C) A serial section of Fig3B. Most of the slug positive cells expressed KIT, suggesting their differentiation to the melanocyte lineage.
(D) A serial section of Fig3BC. A considerable number of the cells surrounding the tube-like structure expressed tyrosinase. The scale bar indicated 20 μm in AB and 10 μm in CD.

and then the cells were further cultured in the N2-supplemented media containing fibronectin and BMP4[17]. The NCCs were efficiently induced by the addition of BMP4, which was evidenced by the emergence of slug and snail expressing cells around the tube-like structures. Here, we cultured the slug positive NCCs for the induction of melanocyte precursors (Fig.1). ES cells were sequentially treated with RA and transferred to the medium including N2-supplement and fibronectin on Day8. BMP4 was added on Day10, 12 and 14. Alternatively, SCF and EDN3 were introduced to the cell culture together with BMP4 on Day10.

mRNA expression of the cell aggregates was analyzed by RT-PCR (Fig.2). As we reported previously, cell aggregates treated by RA and BMP4 expressed slug, a marker of NCCs (Fig.2). From Day 10 they started to express pax3, a marker of neural crest stem cells, and Sox10 and Lef1, essential transcription factors for Mitf expression. Mitf is a product of a master gene to direct the melanocyte differentiation. Expression of c-kit, a receptor for SCF, and EDNRB, that for EDN3, was found during Day 10 and Day14. The cell aggregates expressed Dct, Tryp1 and tyrosinase, all of which were specifically expressed in melanocytes (Fig.2 and Fig.4).

Next, we examined protein expression of slug, KIT and tyrosinase, which are representative markers of melanocyte differentiation. Fig.3A showed a representative section of a cell aggregate treated by RA and BMP4, containing a neural tube-like structure surrounded by NCCs. The NCCs surrounding the tube-like structure expressed slug in their nuclei (Fig.3B). Analyzing serial sections, most of the slug positive cells expressed KIT on their cell membrane (Fig.3C) and a considerable number of the KIT positive cells further expressed tyrosinase in their cytoplasmic region (Fig.3D). Thus, NCCs induced by treating with RA and BMP-4 differentiated to melanocyte precursors (slug and KIT expressing cells), probably receiving signals from SCF produced by the cultured cells, and a considerable population of the melanocyte precursors further differentiated to premature melanocytes (KIT and tyrosinase expressing cells).

It is interesting to study whether the melanocyte precursors derived from ES cells accommodate to and survive in the *in vivo* condition. We thus transplanted the melanocyte precursors into the femoral quadriceps muscle of C57BL/6 mice. ES cells were further treated with SCF and EDN3 in addition to RA and BMP4 to accelerate melanocyte differentiation. Characteristics of the differentiated cells were evaluated by RT-PCR at Day 12 and 14 because the cells were considered to retain abilities of expansion and differentiation in the period. As results, the cells at Day 14 further treated with SCF and EDN3 expressed all the examined molecules which committed to the melanocyte development, thus, they were used for the subsequent transplantation (Fig.4). Five days after the transplantation, the graft was recovered for analysis of the adaptation of the melanocyte precursors *in vivo*. HE staining of the graft disclosed that the cells with high nucleus/cytoplasm ratio made a cluster surrounded by the muscle tissue (Fig.5AB). They were easily distinguished as grafted cells from the host muscle because of their unique histological feature. Some of the cells showing spindle and polygonal shapes seemed to start extending dendrites (Fig.5B). Most of the cells clustering

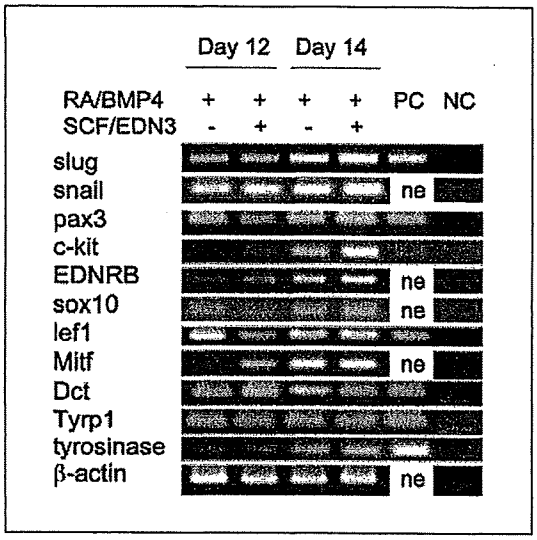

Fig.4 mRNA expressions of the melanocyte precursors induced by RA, BMP4, SCF and EDN3

ES cells were first treated by RA on Day 4 and Day 6, and then treated by BMP-4, SCF and EDN3 on day 10 (see Fig.1). The cells were further cultured up to Day 14. Expression of mRNAs associated with the neural crest and melanocyte differentiation was studied by RT-PCR. PCR templates for positive control study (PC) and negative control study (NC) were NCC-melan5 cDNAs and de-ionized water, respectively. ne, not examined.

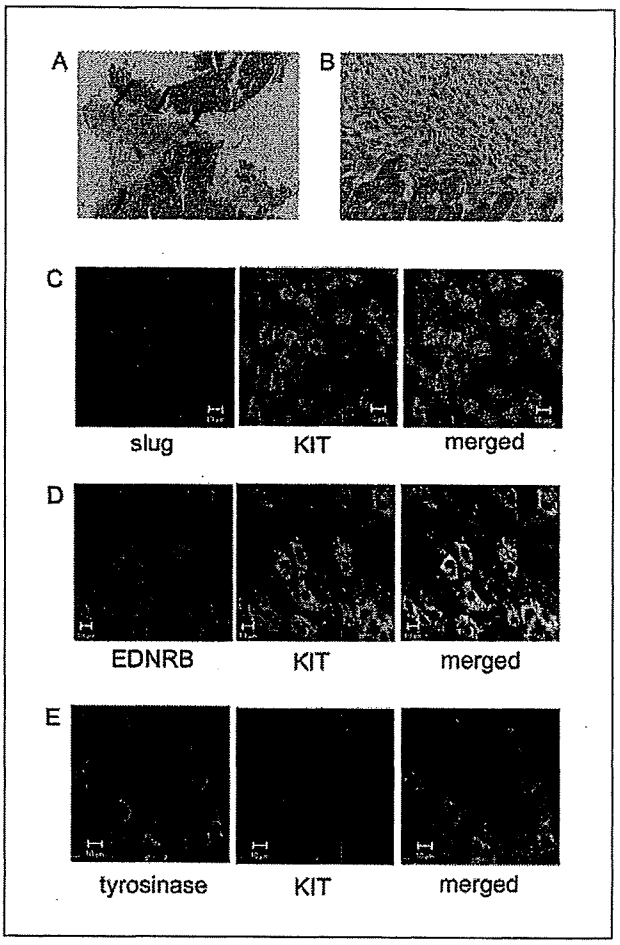

Fig.5 Transplantation of the melanocyte precursors to the femoral quadriceps muscles of recipient mice

Melanocyte precursors derived from ES cells treated with RA, BMP4, SCF and EDN3 (see Fig.4) were injected to femoral quadriceps muscles of C57BL/6 mice. The muscles were recovered five days after the transplantation for the histological examination. Results of HE staining (AB) and two color immunofluorescence staining (CDE) were shown.

(A) HE staining showed relatively homogeneous cells accumulating at the site of transplantation in the muscle tissue. Arrows indicate the boundary of the transplanted site (x 20).

(B) A boundary between the grafted cells and the host muscle tissue. Cells with relatively high nucleus/cytoplasm ratio made a cell cluster in the host muscle tissue and most of them showed spindle or polygonal appearance (x 200).

(C) The transplanted site stained with two color immunofluorescence using antibodies for slug (red) and KIT (green). A number of slug and KIT expressing cells were detected in the grafted region.

(D) Most of KIT expressing cells (green) also expressed EDNRB (red).

(E) A considerable number of KIT expressing cells (red) contained tyrosinase (green), suggesting their differentiation to premature melanocytes.

within the muscle expressed slug, KIT, and EDNRB, indicating that they retained the characteristics of melanocyte precursors in the grafted site (Fig.5CD). A considerable number of the cells expressed tyrosinase, suggesting their differentiation to premature melanocytes (Fig.5E).

Discussion

We have induced melanocyte precursors from NCCs derived from mouse ES cells that had been treated with RA and BMP4. Because slug positive cells expressed KIT and a considerable number of KIT positive cells expressed tyrosinase, we considered that NCCs induced from ES cells further differentiated to melanocyte precursors (the slug and KIT expressing cells) including premature melanocytes (the KIT and tyrosinase expressing cells). After grafting to mouse muscle tissue, the melanocyte precursors developed *in vitro* from ES cells adapted to the *in vivo* condition.

NCCs are derived from the dorsolateral edge of the neural plate and differentiate into various types of cells including melanocytes[19]. Slug and snail, zinc finger transcription factors of the snail family, are known as the earliest response genes to neural crest inducing signals[3]. Overexpression of slug leads to an excess of neural crest derived melanocyte[20], indicating that slug expression is crucial for the neural crest-derived melanocyte induction. Slug expression was found in most of the cells surrounding the neural tube-like structures in the present study, suggesting that slug may promote melanocyte differentiation even in the case from ES cells (Fig.2, Fig.3B and Fig.4).

As a melanocyte-derivative marker, pax3 locates at higher position compared to sox10 in genetic hierarchies of neural crest development[21]. Mutational analyses revealed that pax3 is required to increase numbers of committed melanoblasts or restricted progenitor cells early in development, whereas Mitf affects the survival rate of the melanoblast within and immediately after emigration from the dorsal neural tube[22]. Our neural crest-derived melanocyte precursors expressed pax3, Sox10 and Mitf, indicating that the cells were systematically differentiated, being sequentially influenced by these transcription factors as in somatic developmental procedures. Wnt signaling may also contribute to induction of our melanocyte precursors because they also expressed Lef1.

KIT and its ligand SCF are required to sustain melanocyte development in different stages of embryogenesis during migration, colonization and population of skin[6]. EDNRB is expressed in mouse melanoblasts and its ligand EDN3 works in a paracrine fashion during melanocyte development. Mutation in genes encoding these molecules shows white coat spots due to deficiency of melanocyte differentiation[23-26]. Our melanocyte precursor cells expressed both EDNRB and c-kit, suggesting that they are capable to supply sufficient number of normally differentiating melanocyte precursors by receiving the signals from the ligands.

mRNA expression of a part of examined molecules was also detected in ES cell-derived cDNAs (Fig.2). It sometimes happens that a small portion of ES cells escapes from the undifferentiation-maintaining culture condition and expresses differentiation marker molecules. Such escapes happen very irregularly and not all the differentiation marker molecules associated with a particular directed-differentiation express in such cases as seen in the results of Fig.2. Indeed, once ES cells are transferred to the specific culture condition for inducing a particular directed-differentiation, the expression of differentiation marker molecules in ES cells once disappears and then reappears, and continues thereafter until maturation stages[27].

SCF and EDN3 have been reported to efficiently induce more mature DOPA positive cells and melanocytes from cultures of NCCs[28-32]. Supplementation of SCF and EDN3 to the ES cell culture stimulated with RA and BMP4 promote efficient melanocyte precursors for the transplantation experiments. We reduced the amount of BMP4 in the case of SCF and EDN3 supplementation, considering that excess amount of BMP4 may interfere with the melanocyte differentiation. After transplantation, a large number of cells showed a shape of premature dendritic cells (Fig5B) and expressed slug, KIT and EDNRB (Fig5CD), indicating that they, at least partly shared the characteristics of both NCCs and differentiated melanocyte precursors. The cells expressing KIT and EDNRB were capable of receiving signals from SCF and EDN3, thus, may efficiently maturate to functional melanocytes. Presence of the tyrosinase expressing cells suggested their ability to synthesize melanins (Fig5E). Moreover, mRNA expression of Dct and Tyrp1 was found in the cell aggregates treated with RA and BMP4, and in that further treated with SCF and EDN3 (Fig.4), suggesting that those cell aggregates included highly differentiated melanocytes which have the ability to synthesize eumelanins. In the case of premature melanocytes (KIT and tyrosinase expressing cells) detected at the site of transplantation, they might have acquired the well-differentiated melanocyte characters *in vitro* and retained them even after the transplantation. Otherwise, they may be differentiated from melanocyte precursors after the transplantation. Further studies will be needed to assess this point and to consider which differentiation procedures of cells are more adequate for the cell transplantation.

Several methods for the melanocyte induction have been reported including that from ES cells[33]. An immortal line of melanoblasts was induced from cultures of neonatal mouse epidermis[34]. Mizoguchi et al. established immortal melanocyte precursor cell lines designated as NCCmelan5, NCCmelb4 and NCCmelb4M5 from mouse NCC lines[35-37]. Yamane et al. cocultured ES cells with bone marrow-derived stromal cells and succeeded in the induction of pigmented melanocytes[38]. The induced melanocytes contained abundant stage IV melanosomes, showing the ability of ES cells to terminally differentiate in the melanocytes. ES cell lines expressing the lacZ reporter gene under the control of the Dct promoter were established and they were used for the study of melanocyte differentiation[39].

There were few studies which induced melanocytes from NCCs derived from ES cells. In the present study, we induced melanocyte precursors from NCCs surrounding the neural tube-like structures and successfully transplanted the induced cells to mouse

tissue. We mainly focus KIT expression to detect melanocyte precursors. c-kit expression was detected in NCCs and maintained at high levels until presumptive melanocytes completely differentiate into pigment cells[40]. Luo et al. reported that c-kit and another receptor tyrosine kinase, TrkC, are expressed by distinct neural crest subpopulations and the c-kit expressing NCCs present fate-restricted melanocyte precursors[41]. From this point of view, KIT is a crucial molecule for melanocyte development from NCCs. Further, KIT signaling is indispensable for tyrosinase expression and influences gene expression during melanocyte development[42]. Our KIT expressing cells may be restricted their fate to melanocytes according to somatic development system. KIT expression may be also crucial even for differentiating melanocytes from ES-derived NCCs.

As far as we know, this is the first study to demonstrate successful transplantation of melanocyte precursors induced from ES-derived NCCs. Because differentiation of melanocytes from NCCs is according to somatic development system, our melanocyte precursors have a great advantage of cell transplantation therapy for hypomelanoses such as vitiligo vulgaris[1]. We transplanted the melanocyte precursors to total 8 mice and followed for 5 days after the transplantation. No teratoma fomation was seen in all the cases, however, longer period observation will be required to evaluate the safety of this transplantation. Further studies are needed to elucidate whether our melanocyte precursors differentiate to mature melanocytes to synthesis melanins and whether they retain the function even after transplantation to the site of skin lesion.

References

1) Yu HS: Melanocyte destruction and repigmentation in vitiligo: a model for nerve cell damage and regrowth. J Biomed Sci, 9: 564-573, 2002.
2) Le Douarin NM, Kalcheim C: The Neural Crest. New York, Cambridge University Press, 1999.
3) LaBonne C, Bronner-Fraser M: Molecular mechanisms of neural crest formation. Annu Rev Cell Dev Biol, 15: 81-112, 1999.
4) Relaix F, Rocancourt D, Mansouri A, Buckingham M: Divergent functions of murine Pax3 and Pax7 in limb muscle development. Genes Dev, 18: 1088-1105, 2004.
5) Chi N, Epstein JA: Getting your Pax straight: Pax proteins in development and disease. Trends Genet, 18: 41-47, 2002.
6) Lahav R: Endothelin receptor B is required for the expansion of melanocyte precursors and malignant melanoma. Int J Dev Biol, 49: 173-180, 2005.
7) Watanabe A, Takeda K, Ploplis B, Tachibana M: Epistatic relationship between Waardenburg syndrome genes MITF and PAX3. Nat Genet, 18: 283-286, 1998.
8) Kamaraju AK, Bertolotto C, Chebath J, Revel M: Pax3 down-regulation and shut-off of melanogenesis in melanoma B16/F10.9 by interleukin-6 receptor signaling. J Biol Chem, 277: 15132-15141, 2002.
9) Potterf SB, Furumura M, Dunn KJ, Arnheiter H, Pavan WJ: Transcription factor hierarchy in Waardenburg syndrome: regulation of MITF expression by SOX10 and PAX3. Hum Genet, 107: 1-6, 2000.
10) Elworthy S, Lister JA, Carney TJ, Raible DW, Kelsh RN: Transcriptional regulation of mitfa accounts for the sox10 requirement in zebrafish melanophore development. Development, 130: 2809-2818, 2003.
11) Dorsky RI, Raible DW, Moon RT: Direct regulation of nacre, a zebrafish MITF homolog required for pigment cell formation, by the Wnt pathway. Genes Dev, 14: 158-162, 2000.
12) Larue L, Kumasaka M, Goding CR: Beta-catenin in the melanocyte lineage. Pigment Cell Res, 16: 312-317, 2003.
13) Murisier F, Beermann F: Genetics of pigment cells: lessons from the tyrosinase gene family. Histol Histopathol, 21: 567-578, 2006.
14) Keller G: Embryonic stem cell differentiation: emergence of a new era in biology and medicine. Genes Dev, 19: 1129-1155, 2005.
15) McKinnell IW, Rudnicki MA: Developmental biology: one source for muscle. Nature, 435: 898-899, 2005.
16) Stocum DL: Stem cells in regenerative biology and medicine. Wound Repair Regen, 9: 429-442, 2001.
17) Chiba S, Kurokawa MS, Yoshikawa H, Ikeda R, Takeno M, Tadokoro M, Sekino H, Hashimoto T, Suzuki N: Noggin and basic FGF were implicated in forebrain fate and caudal fate, respectively, of the neural tube-like structures emerging in mouse ES cell culture. Exp Brain Res, 163: 86-99, 2005.
18) Kashiwakura J, Suzuki N, Nagafuchi H, Takeno M, Takeba Y, Shimoyama Y, Sakane T: Txk, a nonreceptor tyrosine kinase of the Tec family, is expressed in T helper type 1 cells and regulates interferon gamma production in human T lymphocytes. J Exp Med, 190: 1147-1154, 1999.
19) Christiansen JH, Coles EG, Wilkinson DG: Molecular control of neural crest formation, migration and differentiation. Curr Opin Cell Biol, 12: 719-724, 2000.
20) LaBonne C, Bronner-Fraser M: Neural crest induction in

Xenopus: evidence for a two-signal model. Development, 125: 2403-2414, 1998.

21) Hou L, Loftus SK, Incao A, Chen A, Pavan WJ: Complementation of melanocyte development in SOX10 mutant neural crest using lineage-directed gene transfer. Dev Dyn, 229: 54-62, 2004.

22) Hornyak TJ, Hayes DJ, Chiu LY, Ziff EB: Transcription factors in melanocyte development: distinct roles for Pax-3 and Mitf. Mech Dev, 101: 47-59, 2001.

23) Russell ES: Hereditary anemias of the mouse: a review for geneticists. Adv Genet, 20: 357-459, 1979.

24) Silvers WK: The coat colors of mice: A model for gene action and interaction. New York, Springer Verlag, 1979.

25) Hosoda K, Hammer RE, Richardson JA, Baynash AG, Cheung JC, Giaid A, Yanagisawa M: Targeted and natural (piebald-lethal) mutations of endothelin-B receptor gene produce megacolon associated with spotted coat color in mice. Cell, 79: 1267-1276, 1994.

26) Baynash AG, Hosoda K, Giaid A, Richardson JA, Emoto N, Hammer RE, Yanagisawa M: Interaction of endothelin-3 with endothelin-B receptor is essential for development of epidermal melanocytes and enteric neurons. Cell, 79: 1277-1285, 1994.

27) Ide M, Ueda Y, Watanabe K, Kurokawa MS, Yoshikawa H, Sakakibara M, Hashimoto T, Suzuki N: Characterization of intracellular free Ca2+ movements in neural progenitor cells derived from ES cells transfected with MASH1 transcription factor gene. Inflamm Regen, 25: 452-460, 2005.

28) Murphy M, Reid K, Williams DE, Lyman SD, Bartlett PF: Steel factor is required for maintenance, but not differentiation, of melanocyte precursors in the neural crest. Dev Biol, 153: 396-401, 1992.

29) Morrison-Graham K, Weston JA: Transient steel factor dependence by neural crest-derived melanocyte precursors. Dev Biol, 159: 346-352, 1993.

30) Lahav R, Ziller C, Dupin E, Le Douarin NM: Endothelin 3 promotes neural crest cell proliferation and mediates a vast increase in melanocyte number in culture. Proc Natl Acad Sci USA, 93: 3892-3897, 1996.

31) Reid K, Turnley AM, Maxwell GD, Kurihara Y, Kurihara H, Bartlett PF, Murphy M: Multiple roles for endothelin in melanocyte development: regulation of progenitor number and stimulation of differentiation. Development, 122: 3911-3919, 1996.

32) Ono H, Kawa Y, Asano M, Ito M, Takano A, Kubota Y, Matsumoto J, Mizoguchi M: Development of melanocyte progenitors in murine Steel mutant neural crest explants cultured with stem cell factor, endothelin-3, or TPA. Pigment Cell Res, 11: 291-298, 1998.

33) Motohashi T, Aoki H, Yoshimura N, Kunisada T: Induction of melanocytes from embryonic stem cells and their therapeutic potential. Pigment Cell Res, 19: 284-289, 2006.

34) Sviderskaya EV, Wakeling WF, Bennett DC: A cloned, immortal line of murine melanoblasts inducible to differentiate to melanocytes. Development, 121: 1547-1557, 1995.

35) Ooka S, Kawa Y, Ito M, Soma Y, Mizoguchi M: Establishment and characterization of a mouse neural crest derived cell line (NCCmelan5). Pigment Cell Res, 14: 268-274, 2001.

36) Watabe H, Soma Y, Ito M, Kawa Y, Mizoguchi M: All-trans retinoic acid induces differentiation and apoptosis of murine melanocyte precursors with induction of the microphthalmia-associated transcription factor. J Invest Dematol, 118: 35-42, 2002.

37) Kawa Y, Soma Y, Nakamura M, Ito M, Kawakami T, Baba T, Sibahara K, Ohsumi K, Ooka S, Watabe H, Ono H, Hosaka E, Kimura S, Kushimoto T, Mizoguchi M: Establishment of a kit-negative cell line of melanocyte precursors from mouse neural crest cells. Pigment Cell Res, 18: 188-195, 2005.

38) Yamane T, Hayashi S, Mizoguchi M, Yamazaki H, Kunisada T: Derivation of melanocytes from embryonic stem cells in culture. Dev Dyn, 216: 450-458, 1999.

39) Pla P, Solov'eva O, Moore R, Alberti C, Kunisada T, Larue L: Dct::lacZ ES cells: a novel cellular model to study melanocyte determination and differentiation. Pigment Cell Res, 17: 142-149, 2004.

40) Lecoin L, Lahav R, Martin FH, Teillet MA, Le Douarin NM: Steel and c-kit in the development of avian melanocytes: a study of normally pigmented birds and of the hyperpigmented mutant silky fowl. Dev Dyn, 203: 106-118, 1995.

41) Luo R, Gao J, Wehrle-Haller B, Henion PD: Molecular identification of distinct neurogenic and melanogenic neural crest sublineages. Development, 130: 321-330, 2003.

42) Hou L, Panthier JJ, Arnheiter H: Signaling and transcriptional regulation in the neural crest-derived melanocyte lineage: interactions between KIT and MITF. Development, 127: 5379-5389, 2000.

Cell Transplantation, Vol. 16, pp. 57–65, 2007
Printed in the USA.

0963-6897/07 $90.00 + .00
E-ISSN 1555-3892
www.cognizantcommunication.com

Plasma as a Scaffold for Regeneration of Neural Precursor Cells After Transplantation Into Rats With Spinal Cord Injury

Mitsuko Takenaga,* Yuki Ohta,* Yukie Tokura,* Akemi Hamaguchi,* Noboru Suzuki,† Masaya Nakamura,‡ Hideyuki Okano,§ and Rie Igarashi*

*Institute of Medical Science, St. Marianna University School of Medicine, Kawasaki 216-8512, Japan
†Department of Immunology and Medicine, St. Marianna University School of Medicine, Kawasaki 216-8512, Japan
‡Department of Orthopaedic Surgery, Keio University School of Medicine, Tokyo 160-8582, Japan
§Department of Physiology, Keio University School of Medicine, Tokyo 160-8582, Japan

The present study investigated whether plasma could be useful as a scaffold for cell transplantation in rats with spinal cord injury (SCI). Transplantation of cells with plasma promoted the recovery of SCI-induced motor dysfunction. Immunohistochemical analysis revealed that the grafted cells had differentiated into the neural lineage. When dissociated neural precursor cells were cultured with plasma, extensive neurite outgrowth was observed along with increased expression of p35 and NF68. Neural markers were also expressed by the cultured cells. Culture with plasma reduced thymidine incorporation, but promoted cell growth and increased the RNA contents. These findings suggest that the cells underwent differentiation into neurons in the presence of plasma. In conclusion, plasma could be a promising scaffold for cell transplantation therapy.

Key words: Neural precursor cell; Plasma; Serum; BBB score; Spinal cord injury

INTRODUCTION

Neural cell transplantation is considered to be a promising therapy for neurodegenerative diseases as well as for trauma such as spinal cord injury (SCI) (20,25). Because embryonic stem (ES) cells differentiate preferentially into neural precursor cells under culture conditions that favor neurogenesis, transplantation of neural precursors derived from ES cells has been reported to promote recovery from SCI-induced motor dysfunction (18).

Scaffolds are considered important to maintain the viability of grafted cells and to promote neural maturation (10,12,24). Hurtado et al. (12) reported that a freeze-dried poly(D,L-lactic acid) macroporous scaffold combined with Schwann cells in a fibrin solution led to production and secretion of brain-derived neurotrophic factor (BDNF) and neurotrophin-3 (NT-3). Prang et al. (21) showed that alginate-based hydrogel combined with adult neural progenitor cells promoted cell contact-mediated axonal regeneration. Scaffolds without any cells have also been reported to induce axonal regeneration (3,13,14,21,22).

Yamada et al. (26) found that platelet-rich plasma (PRP) could enhance the formation of new bone and that it is nontoxic, nonimmunoreactive, and accelerates wound healing. They demonstrated that a combination of PRP (as an autologous scaffold) and culture-expanded mesenchymal stem cells could increase osteogenesis compared with the scaffold alone or autogenous cancellous bone chips and marrow. Yang et al. (27) reported that plasma-treated, collagen-anchored polylactone facilitated cell transplantation and showed improved cellular affinity.

Plasma has various advantages as a scaffold. It contains growth factors that include neurotrophic factors (7,16), fibrinogen, and fibronectin, which are used for neural cell culture. Because autologous plasma can be used, the problem of immune reactions can also be overcome.

We have been investigating cell transplantation therapy after SCI (17,23). The present study was performed to determine whether plasma was potentially useful as a scaffold to promote the survival and differentiation of transplanted neural precursor cells in rats with SCI.

MATERIALS AND METHODS

Differentiation of Embryonic Stem (ES) Cells Into Neural Precursor Cells

Mouse ES cells (R-CMTI-1) were obtained from Dainippon Pharmaceutical Co. (Osaka, Japan) and used

Received May 2, 2006; final acceptance September 8, 2006.
Address correspondence to Mitsuko Takenaga, Ph.D., Institute of Medical Science, St. Marianna University School of Medicine, 2-16-1 Sugao, Miyamae-ku, Kawasaki 216-8512, Japan. Tel: +81-44-977-8111; Fax: +81-44-976-3747; E-mail: m2take@marianna-u.ac.jp

after 12–18 passages. Undifferentiated ES cells were propagated in the presence of leukemia inhibitory factor (LIF, Chemicon Technologies, USA), and then differentiation was induced as follows. Cells were cultured as embryonic bodies (EB) in the absence of LIF for 4 days, after which 1 μM all-*trans* retinoic acid (RA, Sigma Chemical Co., St. Louis, MO, USA) was added on the 4th and 6th days. Treatment of ES cells with RA has already been reported to induce neural differentiation (1,2), and about 80% of RA-treated cells become positive for neural cell adhesion molecule (NCAM) (8). On the 8th day, the cells were dissociated into a single-cell suspension (neural precursor cells) and then were used for the in vitro and in vivo studies. In some experiments, GFP-expressing ES cells were used (19).

Spinal Cord Injury (SCI) and Cell Transplantation

Adult female SD rats weighing 222.7 ± 17.8 g were used to create the SCI model. Under anesthesia, dorsal laminectomy was performed at the T9–10 level. Then a 10-g weight was dropped onto the spinal cord from a height of 25 mm. The Basso/Beattie/Bresnahan (BBB) score (4,5) was determined on the day before cell transplantation. On the 9th day after SCI, neural precursor cells (5×10^6 cells in 5 μl) were transplanted at the site of injury using a Hamilton syringe. Before and after cell transplantation, cyclosporine A (10 mg/kg/day) was injected subcutaneously for 4 days. Blood was collected from each rat on the day of cell transplantation. All animals were housed at a constant temperature (23 ± 1°C) and humidity (50–60%) with free access to a standard diet and water in an animal room with a 12-h light/dark cycle. The study protocol was approved by the Animal Experimentation Committee of St. Marianna University.

Immunohistochemical Analysis

Rats were anesthetized and perfused with 4% paraformaldehyde (pH 7.4) in PBS by intracardiac injection. Then specimens of the spinal cord (1.5 cm long) containing the site of injury were harvested. The following primary antibodies were used for immunohistochemistry: mouse anti-neurofilament 200 (NF200) and mouse anti-βIII tubulin for detection of neurons (Sigma Chemical Co.), mouse anti-glial fibrillary acidic protein (GFAP) for identification of astrocytes (Santa Cruz Biotechnology), and mouse anti-growth-associated protein 43 (GAP43, Zymed Laboratories Inc.). Incubation with the biotin-conjugated secondary antibody was followed by incubation with HRP-conjugated streptavidin, after which visualization was performed with 3,3′-diaminnobenzidine tetrahydrochloride and H_2O_2 in Tris-HCl-buffered saline (pH 7.5). A rhodamine-conjugated secondary antibody was used in some experiments. Fluorescent images were acquired by employing a conventional microscope equipped with a CCD camera (IX71/Cool SNAP-HQ, Olympus, Melville, NY, USA).

Enzyme-Linked Immunoassay

Spinal cord lysates were used for this assay. The primary antibodies were rabbit anti-BDNF (Chemicon Inc.), rabbit anti-glial cell-derived neurotrophic factor (GDNF, Santa Cruz Biotechnology Inc.), and mouse anti-ciliary neurotrophic factor (CNTF, R&D Systems Inc.). Then incubation was done with a biotin-conjugated secondary antibody, followed by incubation with HRP-conjugated streptavidin, after which 0.25% 2,2′-azino bis(3-ethylbenzthiazoline-6-sulfonic acid) (Sigma) was added to each well. The plates were incubated at room temperature, and color development was assessed from the absorbance at 415 nm. Results were expressed as the absorbance per milligram of protein (23).

Morphology

Neural precursor cells were seeded at 1×10^6/well in DMEM containing N2 supplement and fibronectin, and then were cultured at 37°C under a 5% CO_2/95% atmosphere. Subsequently, the cell morphology was observed by phase-contrast microscopy.

Cell Proliferation

Neural precursor cells were seeded at 1×10^5 or 2×10^5/well. After plasma or serum (10%) obtained from 6-week-old C57BL/6 male mice was added to the cells, incubation was done for 24 or 48 h. Then the uptake of [^{3}H]thymidine [methyl, 1′,2′-^{3}H thymidine (1.40 TBq/mmol)] was determined, and the MTT assay was also performed.

RT-PCR Analysis

Quantitative real-time RT-PCR was performed to assess changes in the expression of p35 and neurofilament 68 (NF68). Total RNA was isolated by using ISOGENTM (Nippon Gene, Tokyo, Japan). cDNA was synthesized by using a first-strand cDNA synthesis kit for RT-PCR (AMV)$^+$ (Roche Applied Science) and was labeled with Sybr Green 1 dye. PCR was done by using a Light Cycler System (Roche Molecular Biochemicals) and the following pairs of primers: p35 (PCR product of 923 bp), CGGCACGGTGCTGTCCCTGTCT (forward) and TCACCGATCCAGGCCTAGGAG (reverse); NF68 (327 bp), TGGAGAATGAGCTGAGAAGC (forward) and TTCGTAGCCTCAATGGTCTC (reverse); and G3PDH (452 bp), ACCACAGTCCATGCCATCAC (forward) and TCCACCACCCTGTTGCTGTA (reverse).

Statistical Analysis

Statistical analysis was performed by using the Mann-Whitney *U*-test and $p < 0.05$ was taken to indicate significance.

RESULTS

Neural Precursor Cell Transplantation Into SCI Rats

Rats with neural precursor cell transplantation showed improved movement of their hindlimbs and had significantly higher BBB scores than the SCI control group (Fig. 1), whereas the control group only showed minimal functional recovery. The BBB value was 1.5 ± 0.7 in the SCI control group versus 3.20 ± 0.7 in the cell transplantation group on the 14th day ($p < 0.05$). Rats that received cells plus plasma showed significantly better motor function (6.0 ± 1.10) than SCI controls ($p < 0.05$) and rats with cell grafts alone ($p < 0.05$). Transplantation of cells with serum also promoted functional recovery with a BBB score of 3.5 ± 1.08 on the 14th day, which was significantly higher compared with that of the SCI control group but lower than that of the cells plus plasma group ($p < 0.05$).

Immunohistochemical Findings

Immunohistochemical examination showed that the grafted cells had differentiated into neurons (NF200) and astrocytes (GFAP) (Fig. 2). GAP43 has been used as an index of cell growth status (6,15), and GAP43-positive cells were extensively observed in the spinal cord after grafting of cells plus plasma.

Determination of Neurotrophic Factor

When the levels of BDNF, GDNF, and CNTF in normal spinal cord tissue were set as 100%, SCI reduced these levels to 51.4 ± 5.6%, 59.0 ± 4.0%, and 90.1 ± 5.1%, respectively (Fig. 3). A significant reduction was observed for BDNF and GDNF, but not CNTF. Cell transplantation increased the levels of these neurotrophic factors to 67.1 ± 5.6% for BDNF and 70.2 ± 12.1% for CNTF, while transplantation of cells plus plasma augmented the levels to 90.1 ± 6.6% and 92.2 ± 7.1%, respectively.

Morphological Changes In Vitro

Cells cultured without additives showed slight neurite outgrowth (Fig. 4) and the number of neurites per cell was 1.25 ± 0.6. In contrast, neurite outgrowth in multiple directions (5.25 ± 1.2) was observed in cultures of plasma-treated cells and a gel was formed. The number of neurites was also increased by incubation with serum (5.32 ± 1.3), but the culture medium did not become a gel.

Cell Proliferation

In order to examine whether incubation with plasma affected the proliferation of neural precursor cells, the [^{3}H]thymidine incorporation assay was performed. As shown in Table 1, there was significant suppression of [^{3}H]thymidine uptake by both plasma and serum. In particular, cells cultured with plasma had the lowest uptake of [^{3}H]thymidine and the radioactivity was about one third of the control level after 24 h of incubation with 10% plasma. On the other hand, few apoptotic cells were seen and the MTT assay revealed that there was no adverse influence on cell viability. In fact, cell growth was promoted to some extent. The total RNA

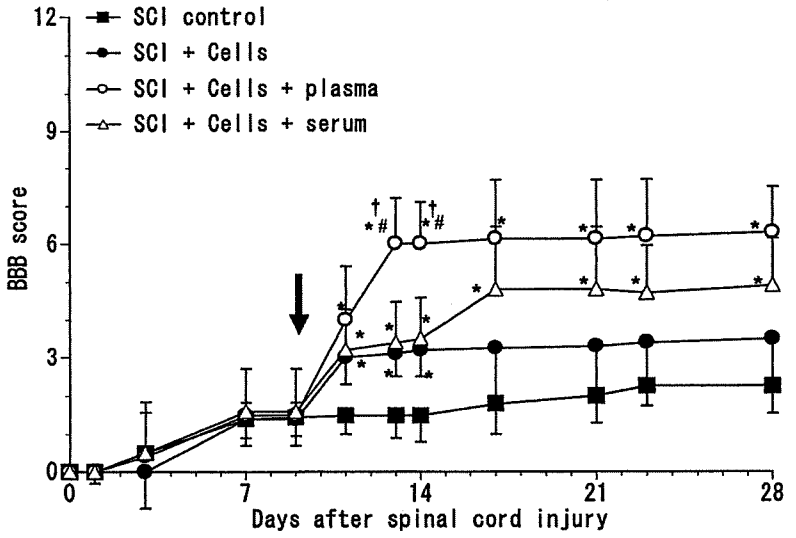

Figure 1. Functional recovery from SCI-induced motor dysfunction following neural precursor cell transplantation with plasma. On the 9th day after SCI (arrow), neural precursor cells (5×10^6) (5 μl) were transplanted at the center of the injured site. BBB scores were monitored before and after cell transplantation (mean ± SD, $n = 6$). *$p < 0.05$ versus the SCI control group, #$p < 0.05$ versus the cell graft group, and †$p < 0.05$ versus the cells plus serum group.

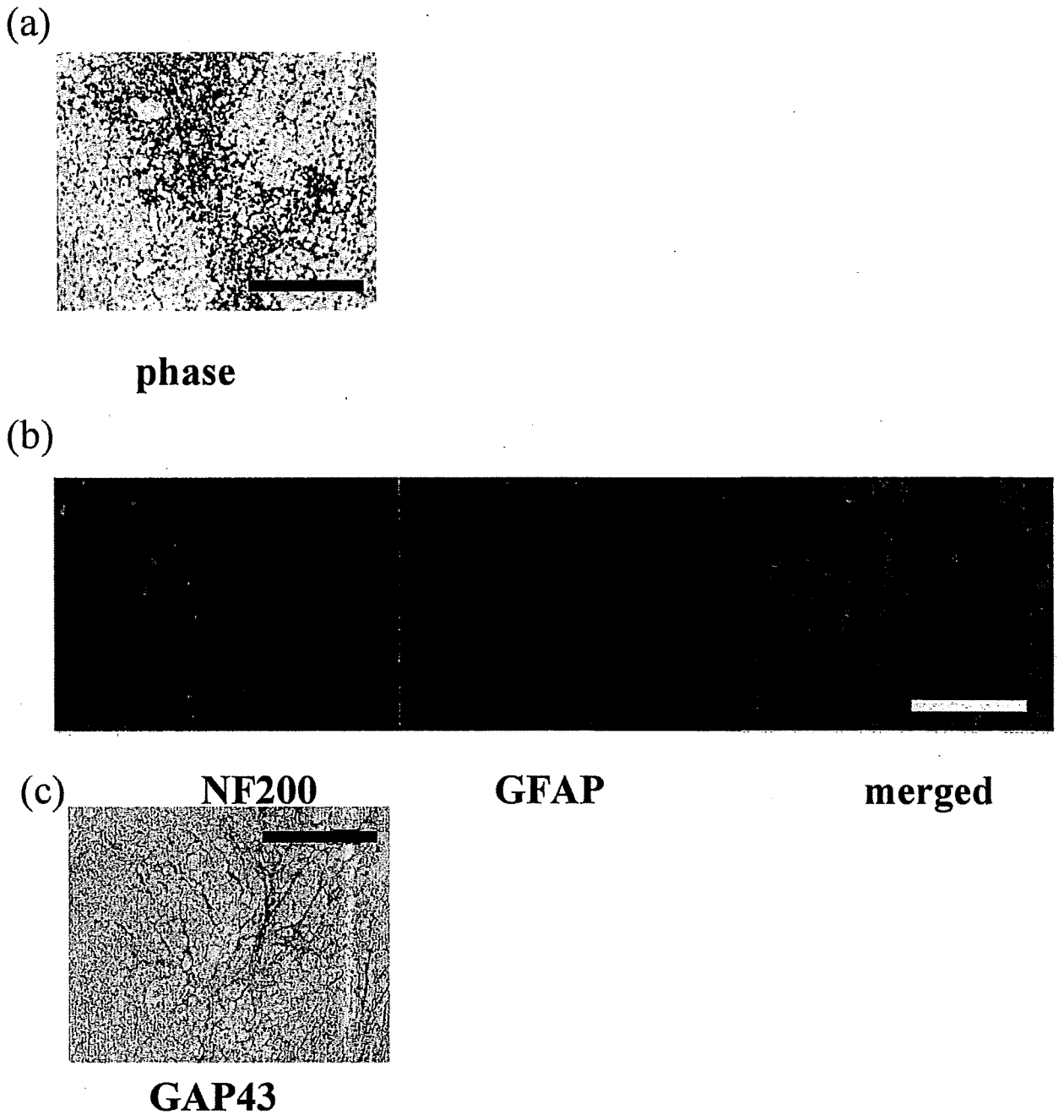

Figure 2. Immunohistochemical staining. The spinal cord from a rat grafted with cells plus plasma was removed at 7 days after cell transplantation for immunohistochemical staining. (a) H&E staining. Scale bar: 100 μm. (b) Cells expressing both NF200 and GFAP. Scale bar: 50 μm. (c) GAP43 expression is extensive. Scale bar: 100 μm.

content showed a slight, but significant increase as well (Table 2).

Neural Gene and Marker Expression In Vitro

Cells positive for βIII tubulin (neurons) and or GFAP (astrocytes) were observed when neural precursor cells that had differentiated from GFP-expressing ES were cultured with plasma (Fig. 5a). Expression of p35 was upregulated by 6.5-fold in the presence of plasma compared with that in cells treated without RA (Fig. 5b). Serum also promoted p35 gene expression by fivefold. Expression of NF68 was upregulated by over 20-fold

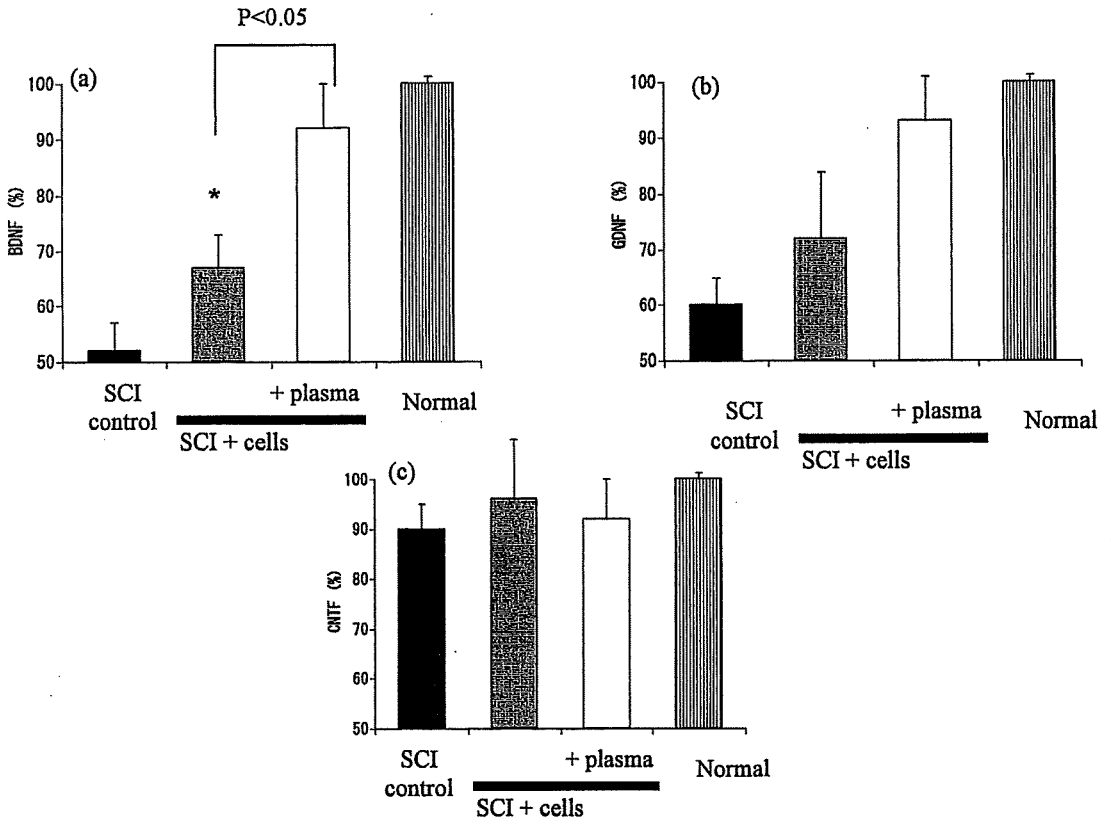

Figure 3. Neurotrophic factor. SCI reduced the levels of neurotrophic factors along with causing cell damage. Antibodies were used for quantification and spinal cords were removed at 7 days after cell transplantation. Values are expressed as a percentage of the control (mean ± SD, $n = 4$).

after addition of plasma to cultures and serum also increased its expression by 19-fold (Fig. 5c).

DISCUSSION

When rats with SCI were monitored using the BBB score, it was shown that cell transplantation promoted functional recovery and this was associated with expression of the axonal growth marker GAP43. It should be noted that transplantation of cells with plasma was more effective than the other methods tested.

Plasma and serum both contain many factors involved in the regulation of cell growth and survival. Chiaretti et al. (7) showed that neurotrophic factors (BDNF, GDNF, and NGF) exist in human plasma, although the levels are lower than in cerebrospinal fluid. Kim et al. (16) reported that the BDNF level in human plasma was 1352.6 pg/ml. Fibronectin, which is used for neural culture, is also found in plasma. In order to survive at the site of transplantation, grafted cells need various cytokines and growth factors. Thus, certain factors might have the potential to promote the cell survival, growth, and differentiation at the graft site. In the present study, plasma might have at least acted as a provider of various factors in the early stage after cell transplantation, in addition to being a scaffold.

Neurotrophic factors, such as BDNF and GDNF, showed an increase in the spinal cord after cell transplantation. The levels of these factors were higher in the cells plus plasma group, indicating that grafted cells had differentiated into neurons after transplantation and then started to secrete these factors. An increase of neurotrophic factors would promote regeneration further. The actions of plasma as a scaffold and provider of neurotrophic factors would have already finished at an earlier stage.

p35 is a neuron-specific activator of cyclin-dependent kinase-5 (cdk5), to which it binds and then triggers neurite sprouting and neurite differentiation in vivo (9). Neurofilaments are the predominant structure in large myelinated axons, where they are considered to function by maintaining the axonal caliber (11). When the cells were cultured with plasma, neurite outgrowth was observed along with increased expression of neural genes and neural markers. Although [^{3}H]thymidine incorpora-